

Experimental and Numerical Study of the Buckling of Composite Profiles with Open Cross Section under Axial Compression

Patryk Rozylo¹ · Andrzej Teter² · Hubert Debski¹ ·
Pawel Wysmulski¹ · Katarzyna Falkowicz¹

Received: 21 December 2016 / Accepted: 12 January 2017

© The Author(s) 2017. This article is published with open access at Springerlink.com

Abstract The object of the research are short, thin-walled columns with an open top-hat cross section made of multilayer laminate. The walls of the investigated profiles are made of plate elements. The entire columns are subjected to uniform compression. A detailed analysis allowed us to determine critical forces and post-critical equilibrium paths. It is assumed that the columns are articulately supported on the edges forming their ends. The numerical investigation is performed by the finite element method. The study involves solving the problem of eigenvalue and the non-linear problem of stability of the structure. The numerical analysis is performed by the commercial simulation software ABAQUS®. The numerical results are then validated experimentally. In the discussed cases, it is assumed that the material operates within a linearly-elastic range, and the non-linearity of the FEM model is due to large displacements.

✉ Andrzej Teter
a.teter@pollub.pl

Patryk Rozylo
p.rozylo@pollub.pl

Hubert Debski
h.debski@pollub.pl

Pawel Wysmulski
p.wysmulski@pollub.pl

Katarzyna Falkowicz
k.falkowicz@pollub.pl

¹ Department of Machine Design and Mechatronics, Lublin University of Technology, Nadbystrzycka 36, 20-618 Lublin, Poland

² Department of Applied Mechanics, Lublin University of Technology, Nadbystrzycka 36, 20-618 Lublin, Poland

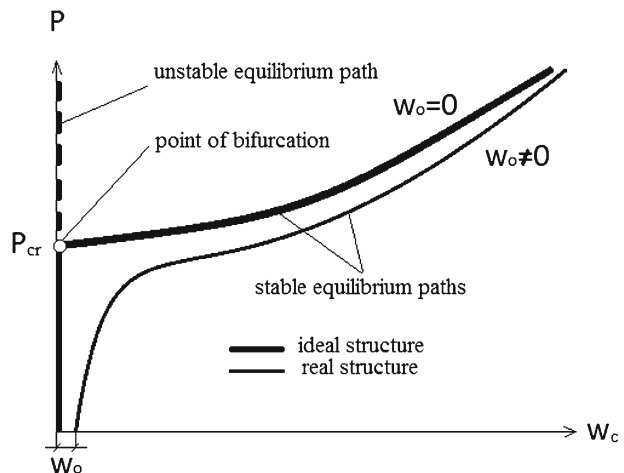
Keywords Critical state · Finite element method · Thin-walled plate structures · Composites · Buckling

1 Introduction

Thin-walled plate structures are basic structural elements for stiffening thin-walled coatings of load-carrying structures. These elements are often exposed to loss of stability even under operationally acceptable loads. In short thin-walled plate structures, the lowest critical load corresponds to local buckling which does not cause damage to these structures. This being the case, when the critical load is exceeded, the element can still operate because the post-critical equilibrium path is stable and symmetric [1–4]. This means that the increase in wall deflection involves an increase in compressive load both for the positive and negative total deflection (Fig. 1, [5]). Figure 1 shows typical post-critical equilibrium paths for an ideal structure without defects, i.e., $w_0 = 0$, and for a real structure, i.e., $w_0 \neq 0$. The vertical axis shows the force causing uniform compression (denoted as P), while the horizontal axis shows the total deflection w_c . One can distinguish three stages in the operation of an ideal plate structure. First, in the pre-critical stage ($P < P_{cr}$) the structure's walls are only compressed and the deflection w_c resulting from bending are equal to zero (membrane state). The second stage involves loss of stability of the structure under critical loads ($P = P_{cr}$) corresponding to the point of bifurcation. Finally, in the post-critical stage ($P > P_{cr}$), when the critical load is exceeded, the deflection w_c caused by bending increases. The real structure shows no presence of bifurcation, so the direct determination of the critical force P_{cr} is impossible. The structure's walls begin to undergo bending from the very beginning of the loading process.

The problem of stability of thin-walled structures under operational static loads was investigated for instance in [6–14], where the authors analyse the operation of thin-walled structures with complex open and closed cross sections. They offer a solution to the problem of non-linear stability of the investigated thin-walled structures using experimental and numerical methods [15–20]. The investigations of critical and post-critical states as well as the damage of thin-walled composite columns are reported, for instance, in the works [6, 7, 14, 15, 21–28], where the authors present different methods for describing the problem of nonlinear stability

Fig. 1 Post-critical equilibrium paths of a plate without initial deflections and of a real structure



and validate the developed numerical models in the experimental tests. In addition, an attempt was made to describe composite material damage by different criteria of composite damage.

As mentioned above, load-carrying plate structures can also operate after stability loss. Due to practical reasons, it is vital to determine the load corresponding to the critical load of real structures. In such a case, bifurcation does not occur and the critical load cannot be determined in a direct way. To this end it is necessary to use approximation methods which – based on the post-critical equilibrium paths of a real structure determined in the experiments – enable determination of the critical load. This problem was examined regarding structures made of isotropic materials, for instance, in the work [10, 24], and with respect to composite structures in the works [5, 7, 27, 28]. They do not offer, however, a complex procedure which would enable developing an unequivocal methodology for determining the experimental critical load.

This study attempts to determine an approximated value of the critical load for the thin-walled composite columns with a top-hat section under axial compression. The literature reports several methods for determining approximated critical forces in real structures, including Southwell's method, [29] vertical tangent [5], line intersection method [30], inflection point method [5], Tereszowski method [31], $P-w_c^2$ and $P-w_c^3$ methods [5], and the Koiter method [32]. In this study, the critical load of the compressed composite columns is determined by the methodology based on Koiter's theory and the methods $P-w_c^2$ and $P-w_c^3$. The critical load values determined in the experiments are compared with the results of the linear numerical calculations (eigenproblem solution) performed by the finite element method.

2 Object of the Study

The study was conducted on thin-walled composite columns with top-hat sections. The columns were 80x40x20 mm and had a length of 180 mm (Fig. 1). The walls of the columns were flat and had small indefinite initial deflection. The specimens were made of a unidirectional carbon/epoxy composite tape symmetrically arranged to the central plane by the autoclave method. The experimentally determined (according to the relevant ISO standard) mechanical properties of a single laminate layer were as follows: Young modulus in the fibre direction $E_1 = 130.71$ GPa, Young modulus perpendicular to fibre direction $E_2 = 6.36$ GPa, Poisson's ratio in the layer plane $\nu_{12} = 0.32$, Kirchhoff's modulus $G_{12} = 4.18$ GPa. The real model of the top-hat section profile and the geometrical model along with the basic dimensions of the structure are shown in Fig. 2.

The walls of the tested top-hat section columns had 8 laminate layers with the lay-up: $[90/-45/45/0]_S$. The total thickness of individual walls of the profile was 1.048 mm. The application of the autoclave technique enabled obtaining high repeatability and quality of the produced composite structures, which had a positive effect on the experimental results.

3 Experimental Tests

The post-critical equilibrium paths of real structures were determined in the experiments using the Zwick Z100 testing machine. The experiments were conducted in room temperature at a constant speed of the upper cross beam set to 2 mm/min. The range of total compressive load was approximately 150% of the predicted critical load determined in numerical analysis. The value of the applied critical load enabled to produce a clear mode of deformation corresponding

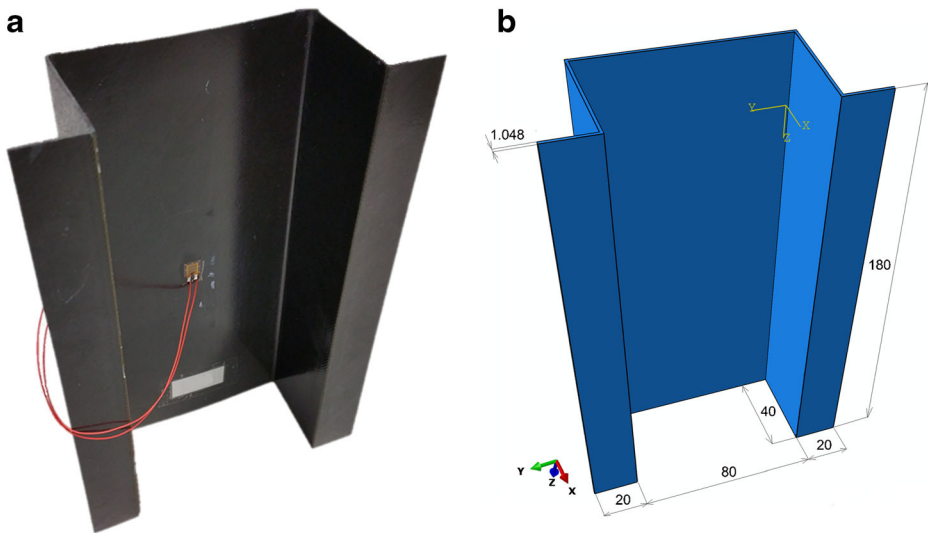
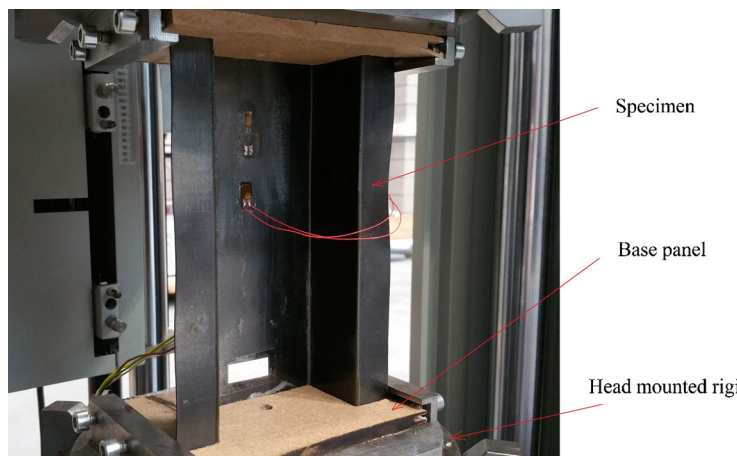


Fig. 2 Column with a top-hat section: (a) specimen, (b) geometrical model and the structure dimensions

to local buckling of the column's walls, which manifested itself in a specified number of half-waves lengthwise to the column. As for the tested load range, we did not observe any shifting between different modes of local buckling or damages to the columns. Preliminary assessment of damage was performed by organoleptic methods and by acoustic emission method. Strains in the direction of load (denoted as, ε_1 and ε_2) were measured using strain gauges located on the opposite sides of the web of the top-hat section profile, in the region of the highest half-wave amplitude determined by numerical analysis. In the tests, the profile ends were simple-supported to ensure articulate support of individual profile walls which had the form of plate elements. To prevent the impact of the boundary conditions on the structure, both ends of the profile were provided with soft material pads to level potential inaccuracies of the end sections of the profile. Individual specimens were aligned using special pads enabling precise setting of the profile's end sections relative to the bolts of the testing machine. The test stand used in the experiments is shown in Fig. 3.

Fig. 3 Test stand



The experiments were performed on three specimens of profiles with a top-channel section described by the same conditions of axial compression of the structure. The experimental tests enabled us to determine post-critical equilibrium paths which were then used to determine an approximated value of critical load using 3 independent approximation methods: the Koiter method and the $P-w_c^2$ and $P-w_c^3$ methods.

Regarding a single-mode buckling for the Koiter method for the second order approximation [12, 13, 32], the post-critical equilibrium path is described by the function:

$$\left(1 - \frac{P}{P_{cr}}\right)\bar{w} + b_{111}\bar{w}^2 + c_{1111}\bar{w}^3 = \frac{P}{P_{cr}}\bar{w}_0$$

where: $\bar{w} = w/h$ is the dimensionless amplitude of the buckling mode (w - maximum deflection referred to the thickness of the structure), P_{cr} , $\bar{w} = w/h$ are the critical load and dimensionless amplitude of the initial deflection corresponding to buckling mode (w - maximum initial deflection referred to the thickness of the structure), b_{111} is the non-linear coefficient in the first order approximations, c_{1111} is the non-linear coefficients in the second order approximations. Assuming that the initial deflection is insignificant, the above formula can be written in a non-dimensional form:

$$\left(1 - \frac{P}{P_{cr}}\right)\bar{w} + b_{111}\bar{w}^2 + c_{1111}\bar{w}^3 = 0$$

or in a dimensional form:

$$P = P_{cr} + \frac{P_{cr}b_{111}}{h}w + \frac{P_{cr}c_{1111}}{h^2}w^2$$

In the Koiter method for the second order approximation [32], the post-critical equilibrium path is described by a quadratic function. As for the experimental results, the values of strains ϵ_1 and ϵ_2 enable to determine the deflection w in the following way:

$$w \sim \epsilon_1 - \epsilon_2 \text{ or } w = k(\epsilon_1 - \epsilon_2)$$

where: k is the coefficient of proportionality.

Substituting the above experimental dependence, the post-critical equilibrium path can be written as:

$$P = P_{cr} + \alpha_1(\epsilon_1 - \epsilon_2) + \alpha_2(\epsilon_1 - \epsilon_2)^2$$

where α_1 and α_2 are unknown constants.

In this case, the experimental critical load is described as a place of intersection between a function described by the above formula and the vertical axis of the coordinate system of the diagram $P = f_1(\epsilon_1 - \epsilon_2)$. All constants in the above equation are determined by the approximation methods for the experimental post-critical equilibrium path $P - (\epsilon_1 - \epsilon_2)$. The accuracy of determination of the critical load depends on the selection of a measuring range and approximation method. In addition, it must be remembered that for the stable equilibrium path the coefficient α_2 must be positive.

With the $P-w_c^2$ and $P-w_c^3$ methods the critical load is also determined based on the post-critical equilibrium path. Nonetheless, the determination of approximate critical load is based on the diagram of load in a function of square difference in strains ($P-w_c^2$ method) or in a function of cubic difference in strains ($P-w_c^3$ method). Regarding the discussed methods, the

post-critical equilibrium paths $P-w_c^2$ and $P-w_c^3$ are approximated by the linear function [5]. In both methods, the critical load is defined as the point of intersection between the determined approximation line and the vertical axis of the coordinate system of the diagram $P = f_2(\varepsilon_1 - \varepsilon_2)^2$ and $P = f_3(\varepsilon_1 - \varepsilon_2)^3$. The results obtained by approximation with the above methods are not always unequivocal. The degree of linearity of the approximated curve strongly depends on the range of data used for determining critical loads. In addition to this, the results significantly depend on the number of points with specified coordinates subjected to approximation.

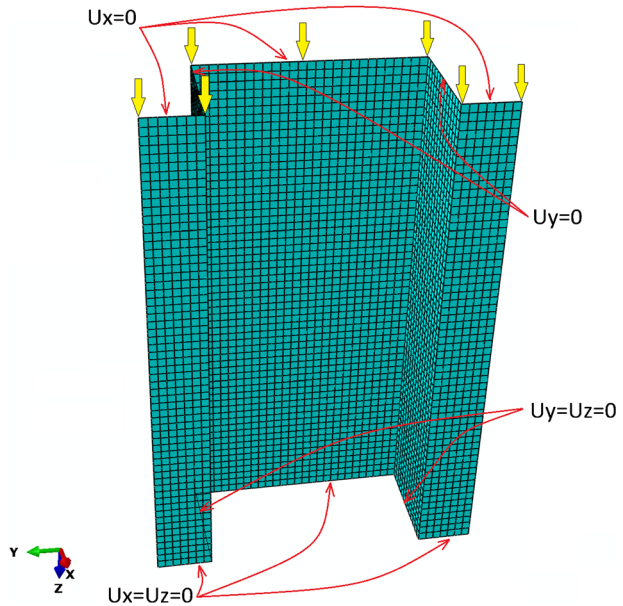
In this study, the correlation ratio R^2 was the key factor responsible for the accuracy of approximation. The value of this ratio determined the level of convergence between the approximation function and the selected range of the approximated experimental curve. In the applied approximation processes for experimental post-critical equilibrium paths of the structure the correlation ratio was set to a minimal value of $R^2 \geq 0.95$.

4 FEM Numerical Analysis

The numerical analysis was conducted by the finite element method using the commercial ABAQUS® simulation software. The scope of the numerical computations involved performing analyses of both critical and weakly post-critical states up to a value of approx. 150% of the lowest determined critical force. The analysis of the critical state involved solving a linear eigenproblem in compliance with the so-called limited approach to bifurcation stability loss based on the criterion of minimal potential energy of the system. The computations enable determination of the lowest critical load and its corresponding buckling mode. The second stage of computations involved a nonlinear static analysis of a model with initiated geometrical imperfection reflecting the lowest buckling mode with an amplitude of 0.1 of the profile wall thickness. This enabled determination of the post-critical equilibrium path of the structure in a weakly post-critical state. The solution of the geometrically non-linear problem for large displacements was performed by the Newton-Raphson method [22, 33, 34]. The discretization of the investigated structure was performed using *SHELL* finite elements. These elements have six degrees of freedom in each node. The discretization process was performed using 8-node shell element with reduced integration, *S8R*. The reduced integration technique enable removing false modes of deformation of finite elements due to the application of higher order polynomials in the definition of a finite element function [35]. The applied multi-layer element enabled the modelling of composite structure by independent definition of layer arrangement and their properties in the element's structure. The discrete model was built using a structural square finite element mesh. The side of a single element was 2 mm, which ensured a uniform division of individual walls of the profile by a mesh with constant density. A general view of the discrete model of the structure is shown in Fig. 4.

The boundary conditions formulated for the numerical model ensured articulated support of the compressed composite columns (Fig. 4). The boundary conditions were ensured by applying zero displacements to the nodes located on the edges of the lower and upper sections of the column, perpendicularly to the plane of each wall (displacements $u_x = 0$ and $u_y = 0$). In addition, the nodes from the bottom end of the column were blocked to prevent vertical displacement ($u_z = 0$), while the nodes belonging to the edge of the top end of the column were described by the same displacement $u_z = const$ via coupling the displacements relative to the axis of the column. The numerical model was subjected to load applied to the edge of the upper section of the column, which ensured uniform compression of the column in the axial

Fig. 4 Discrete model of a thin-walled column with top-hat section



direction. The composite material is described by the properties of orthotropic material in a two-dimensional state of strain, the main orthotropic directions corresponding to the directions of fibre arrangement in the laminate layer. The computations were performed using the experimentally determined mechanical properties of the composite.

5 Results and Discussion

The experimental tests and numerical computations led to determination of critical forces and post-critical equilibrium paths (in a weakly post-critical range) of thin-walled top-hat section profiles under compression. The aim of the study was to determine the critical load of a real structure based on experimental tests performed to determine the relationship between the applied compressive load and strains at selected points of the column. The detailed computations were performed by approximation methods. The key of this approach lies in the use of approximation and selection of a measuring range to describe a post-critical path, which has a direct effect on the results. If the selected approximation procedures are wrong, critical loads significantly differ from the numerical results. The method for determining critical loads (free terms in the equations of approximation functions) depending on the applied approximation range is illustrated in Fig. 5. In Fig. 5, the solid line marks an example of the experimental equilibrium path describing the tested column. In this case, the path is stable. It should also be stressed that this case is characterized by the occurrence of undetermined initial deflection. Given the applied production method and specimen preparation, the initial deflection was assumed to be low, while other manufacturing defects such as shape defects or dimensional inaccuracies are insignificant.

The approximation functions marked in Fig. 5 as 1 (the measuring range for approximation is too short) and 2 (the section for approximation is too long) in the above two cases show

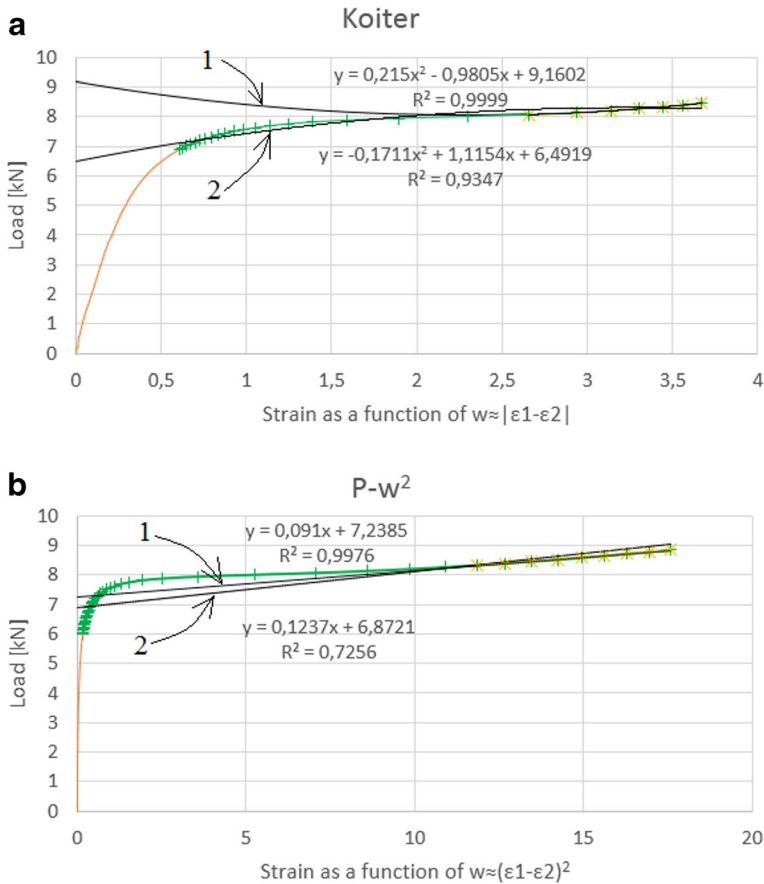
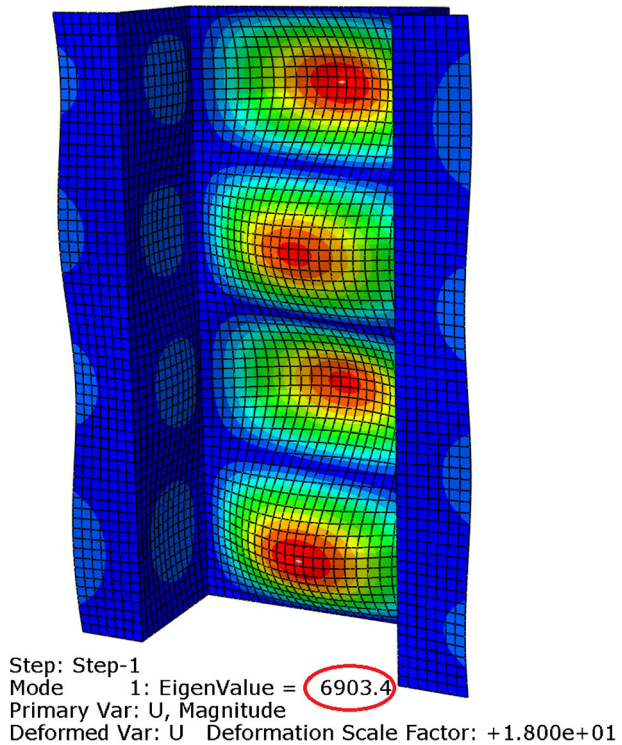


Fig. 5 Effect of selecting measuring range of the approximation process on critical loads: (a) Koiter method, (b) $P-w_c^2$ method

wrong values of the determined critical load. In addition to this, contrary to the assumptions, the post-critical paths determined by the approximation methods reveal non-stable intervals. Also, the selected approximation range should ensure maintaining the highest possible correlation ratio R^2 describing the matching accuracy of the approximation function to the experimental curve. In the numerical simulations we determined that the range of the approximated experimental curve in all investigated cases included a part of the experimental post-critical path which starts at the point of intersection of the *force – strain* line until the end of the curve experimentally determined for a weakly post-critical state (Koiter method) or a linear state ($P-w_c^2$ method), while at the same time maintaining a high correlation ratio ($R^2 > 0.95$). The critical loads determined by the approximation methods were compared with the lowest eigenvalues obtained in the numerical analysis of the eigenproblem defined for the compressed composite profiles. The scope of the linear numerical analysis enabled here the determination of critical load and the corresponding mode of the structure's deformation (eigenmode) based on the criterion of minimal potential energy of the system. The lowest mode of stability mode and its corresponding eigenvalue in the form of a local buckling of the profile walls created by four lengthwise half-waves are shown in Fig. 6.

Fig. 6 Lowest local buckling mode of the top-hat section profile



The critical load results obtained with approximation processes by the Koiter method [5, 32] in axial compression tests are given in Fig. 7.

In a similar way, we determined critical loads corresponding to the lowest buckling mode of the top-hat channel section profile using the $P-w_c^2$ method. To this end, we also employed the approximation method $P-w_c^3$. The approximation of the experimental curve applied in these cases is illustrated in Figs. 8 and 9.

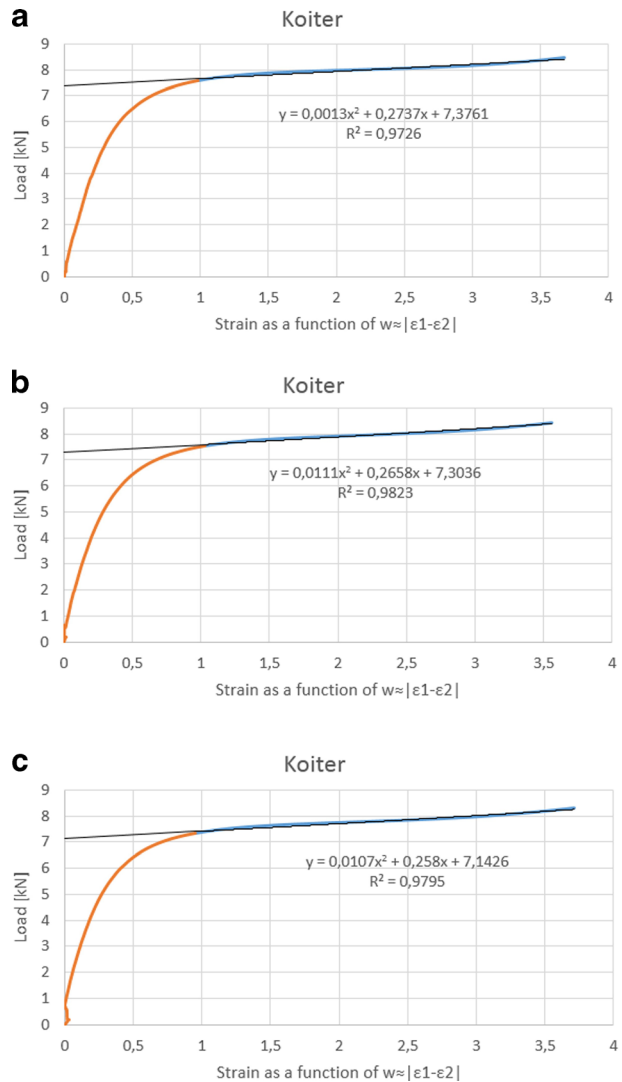
The employed methodology enabled to determine critical loads in experimental tests performed using three independent approximation methods. In all applied methods, the critical load was determined with the free term in the approximation function. Based on the results, we can determine the moment when the structure's operation changes from the membrane state to the flexural (post-critical) state. The above critical forces determined in the physical model compression tests performed on a test stand are compared with the FEM results (Table 1). The values of errors for the experimental critical loads are determined from the following dependence:

$$\delta P_{cr}^* = \frac{|P_{cr}^* - P_{cr}|}{P_{cr}} 100\%$$

where: P_{cr} is the numerical bifurcation load determined by FEM and P_{cr}^* is the experimental critical load.

Examining the data listed in Table 1, we can observe that the results obtained with the Koiter method show a very high agreement with the experimental and FEM numerical results. In addition, the method is very sensitive in terms of performing the approximation process,

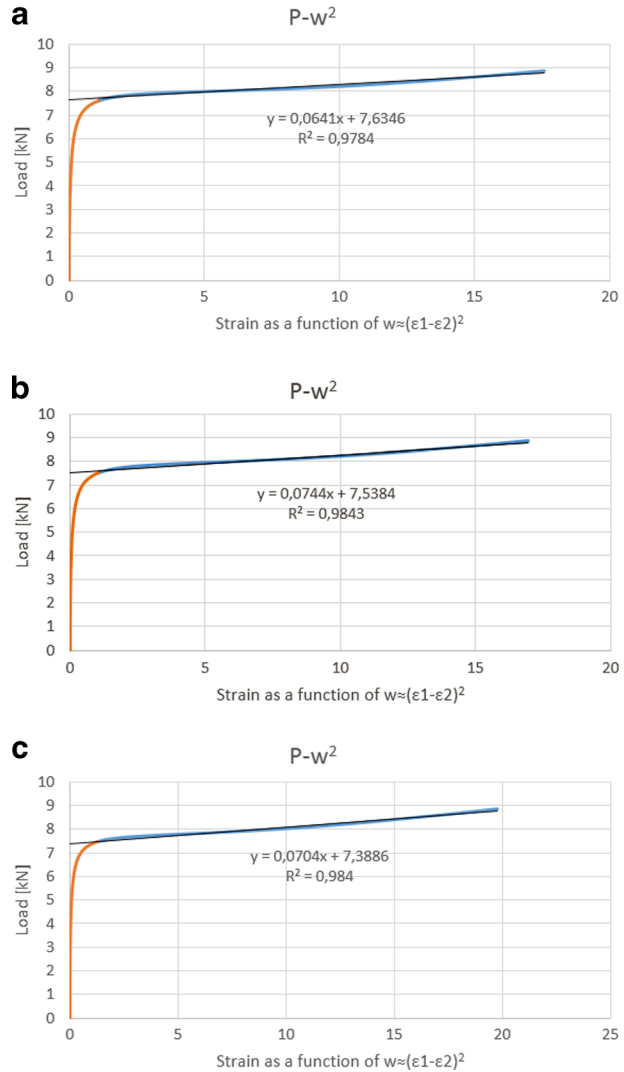
Fig. 7 Experimental post-buckling path and approximation line used for determining critical load by Koiter method: **(a)** test 1, **(b)** test 2, **(c)** test 3



particularly with respect to the selection of curve matching range. The highest difference between the results obtained with the Koiter method and the FEM results does not exceed 6.5%. Higher discrepancies were obtained for the remaining two approximation methods: $P-w_c^2$ – difference: 9.58%, and $P-w_c^3$ – difference: approx. 11.2%.

In addition, we compared the post-critical equilibrium paths $P-w_c$ (compressive force – maximum deflection perpendicular to the profile wall) determined in the weak post-critical range. The paths given in Fig. 10 show qualitative and quantitative agreement with the curve determined on the numerical simulations performed by the finite element method. The results reveal agreement between the experimental findings of the experimental tests and the adequacy of the developed numerical model regarding the critical and post-critical states of composite columns with top-hat sections under compression.

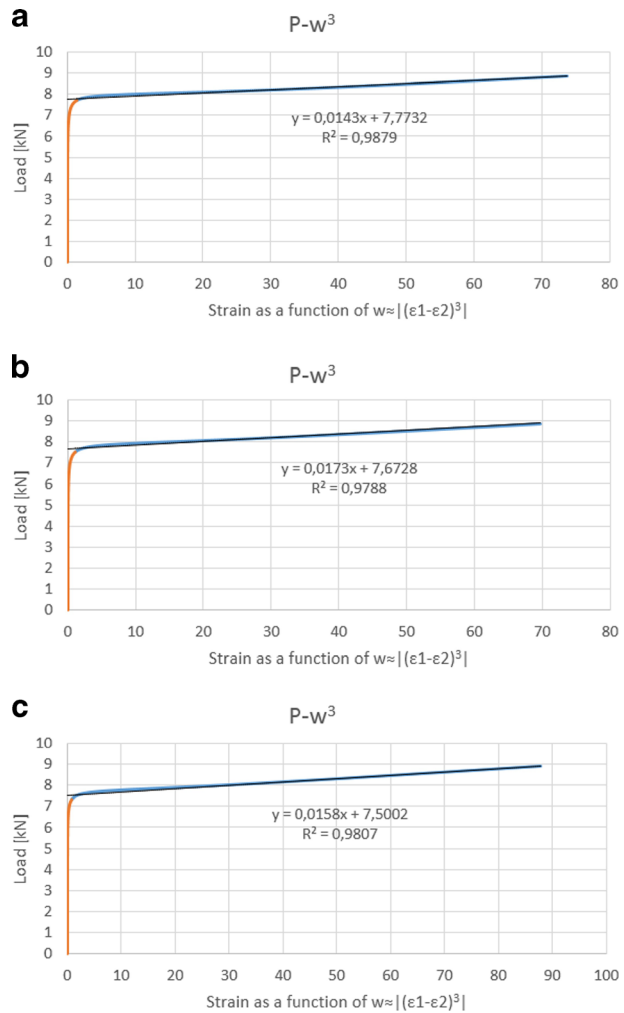
Fig. 8 Experimental results and approximation lines used for determining critical load by $P-w_c^2$ method: **(a)** test 1, **(b)** test 2, **(c)** test 3



6 Conclusions

The paper investigated the critical and post-critical states of thin-walled carbon/epoxy laminate profiles with top-hat sections under compression. The study determined the critical load based on post-critical equilibrium paths determined in the experimental tests performed by 3 independent approximation methods: the Koiter method and the $P-w_c^2$ and $P-w_c^3$ methods. The results showed a high agreement between the critical load results obtained with these approximation methods. The highest results discrepancies do not exceed 11.2% (Specimen 1 - $P-w_c^3$ method). The results reveal a strong correlation between approximation parameters and results accuracy. In particular, this regards the selection of an approximation range and the necessity to obtain a high correlation ratio R^2 to ensure agreement between the experimental characteristics of the structure and the approximation function.

Fig. 9 Experimental results and approximation straight lines used for determining critical load by $P-w_c^3$ method: **(a)** test 1, **(b)** test 2, **(c)** test 3



The critical load results determined in the experimental tests were compared with the results of critical force determined by the linear numerical analysis of eigenproblem. The discrepancies in the critical load results were as follows: Koiter method – 6.5%, $P-w_c^2$ method - 9.6% and $P-w_c^3$ method – 11.2%, which leads to a satisfactory agreement between the results obtained with the applied approximation methods and the numerical findings. Therefore, the applied procedures can help

Table 1 Critical loads – comparison of experimental and numerical results

Specimen no.	FEM	Koiter method		$P-w^2$ method		$P-w^3$ method	
	P_{cr} [N]	P_{cr}^* [N]	δP_{cr}^* [%]	P_{cr}^* [N]	δP_{cr}^* [%]	P_{cr}^* [N]	δP_{cr}^* [%]
1	6903.4	7376.1	6.41	7634.6	9.58	7773.2	11.19
2		7303.6	5.48	7538.4	8.42	7672.8	10.03
3		7142.6	3.35	7388.6	6.57	7500.2	7.96

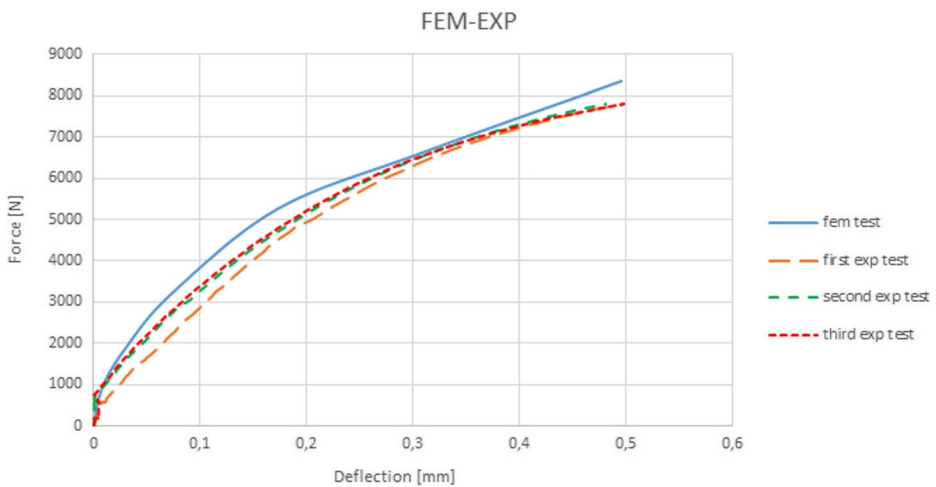


Fig. 10 Comparison of weakly post-buckling equilibrium paths

establish a general methodology of determining critical load of physical structural models, this knowledge being crucial to the operation of thin-walled load-carrying structural elements.

In addition, the comparison of the post-critical equilibrium paths of the structure showed a high agreement of the numerical and experimental results, which confirms the correctness of the developed discrete model of the structure. The results provide essential information with respect to the modelling of thin-walled structures made of composite materials.

Open Access This article is distributed under the terms of the Creative Commons Attribution 4.0 International License (<http://creativecommons.org/licenses/by/4.0/>), which permits unrestricted use, distribution, and reproduction in any medium, provided you give appropriate credit to the original author(s) and the source, provide a link to the Creative Commons license, and indicate if changes were made.

References

1. Bloom, F., Coffin, D.: Handbook of Thin Plate Buckling and Postbuckling. Chapman & Hall, Boca Raton (2001)
2. Magnucka-Blandzi, E., Magnucki, K.: Buckling, and optimal design of cold-formed thin-walled beams: review of selected problems. *Thin-Walled Struct.* **49**, 554–561 (2011)
3. Hancock, G.J.: Cold-formed steel structures. *J. Constr. Steel Res.* **59**, 473–487 (2003)
4. Bazant, Z.P., Cedolin, L.: Stability of Structures. Elastic, Inelastic, Fracture and Damage Theories. Oxford University Press, UK (2010)
5. Paszkiewicz, M., Kubiak, T.: Selected problems concerning determination of the buckling load of channel section beams and columns. *Thin-Walled Struct.* **93**, 112–121 (2015)
6. Debski, H., Teter, A., Kubiak, T., Samborski, S.: Local buckling, post-buckling and collapse of thin-walled channel section composite columns subjected to quasi-static compression. *Compos. Struct.* **136**, 593–601 (2016)
7. Debski, H., Teter, A., Kubiak, T.: Numerical and experimental studies of compressed composite columns with complex open cross-sections. *Compos. Struct.* **118**, 28–36 (2014)
8. Falkowicz, K., Mazurek, P., Rozylo, P., Wysmulski, P., Smagowski, P.: Experimental and numerical analysis of the compression of a thin-walled composite plate. *Adv. Sci. Technol. Res. J.* **10**(31), 177–184 (2016)
9. Kolakowski, Z., Teter, A.: Static interactive buckling of functionally graded columns with closed cross-sections subjected to axial compression. *Compos. Struct.* **123**, 257–262 (2015)
10. Rozylo, P., Wrzesinska, K.: Numerical analysis of the behavior of compressed thin-walled elements with holes. *Adv. Sci. Technol. Res. J.* **10**(31), 199–206 (2016)

11. Taheri, F., Nagaraj, M., Khosravi, P.: Buckling response of glue-laminated columns reinforced with fiber-reinforced plastic sheets. *Compos. Struct.* **88**, 481–490 (2009)
12. Teter, A., Kolakowski, Z.: Buckling of thin-walled composite structures with intermediate stiffeners. *Compos. Struct.* **69**, 421–428 (2005)
13. Teter, A., Kolakowski, Z.: Load carrying capacity of functionally graded columns with open cross-sections under static compression. *Compos. Struct.* **129**, 1–7 (2015)
14. Wyslowski, P., Debski, H., Rozylo, P., Falkowicz, K.: A study of stability and post-critical behaviour of thin walled composite profiles under compression. *Eksploracja i Niezawodność – Maintenance and Reliability.* **18**(4), 632–637 (2016)
15. Doyle, J.F.: *Nonlinear Analysis of Thin-Walled Structures*. Springer, New York (2001)
16. Singer J, Arboez J, Weller T (1998) Buckling experiments. *Experimental methods in buckling of thin-walled structure. Basic concepts, columns, beams, and plates. vol. 1*. New York, Wiley (2002)
17. Becque, J., Rasmusen, K.J.R.: Experimental investigation of local-overall interaction buckling of stainless steel lipped channel columns. *J. Constr. Steel Res.* **65**, 1677–1684 (2009)
18. Turvey, G.J., Zhang, Y.: A computational and experimental analysis of the buckling, postbuckling and initial failure of pultruded GRP columns. *Comput. Struct.* **84**, 1527–1537 (2006)
19. Parlapalli, M.R., Soh, K.C., Shu, D.W., Ma, G.: Experimental investigation of delamination buckling of stitched composite laminates. *Compos. Part A.* **38**, 2024–2033 (2007)
20. Wong, P.M.H., Wang, Y.C.: An experimental study of pultruded glass fibre reinforced plastics channel columns at elevated temperatures. *Compos. Struct.* **81**, 84–95 (2007)
21. Banat, D., Mania, R.J.: Comparison of failure criteria application for FML column buckling strength analysis. *Compos. Struct.* **140**, 806–815 (2016)
22. Debski, H.: Experimental investigation post-buckling behaviour of composite column with top-hat cross section. *Eksploracja i Niezawodność – Maintenance and Reliability.* **2**, 105–109 (2013)
23. Debski, H., Sadowski, T.: Modelling of microcracks initiation and evolution along interfaces of the WC/Co composite by the finite element method. *Comput. Mater. Sci.* **83**, 403–411 (2014)
24. Falkowicz, K., Ferdynus, M., Debski, H.: Numerical analysis of compressed plates with a cut-out operating in the geometrically nonlinear range. *Eksploracja i Niezawodność – Maintenance and Reliability.* **17**(2), 222–227 (2015)
25. Kopecki, T., Mazurek, P.: Numerical representation of post-critical deformations in the processes of determining stress distributions in closed multi-segment thin-walled aircraft load-bearing structures. *Eksploracja i Niezawodność – Maintenance and Reliability.* **16**(1), 164–169 (2014)
26. Kopecki, T., Mazurek, P.: Problems of numerical bifurcation reproducing in postcritical deformation states of aircraft structures. *J. Theor. Appl. Mech.* **51**(4), 969–977 (2013)
27. Mania, R.J., Kolakowski, Z., Bienias, J., Jakubczak, P., Majerski, K.: Comparative study of FML profiles buckling and postbuckling behaviour under axial loading. *Compos. Struct.* **134**, 216–225 (2015)
28. Teter, A., Debski, H., Samborski, S.: On buckling collapse and failure analysis of thin-walled composite lipped-channel columns subjected to uniaxial compression. *Thin-Walled Struct.* **85**, 324–331 (2014)
29. Roorda, J.: Some thoughts on the Southwell plot. *Proc. ASCE. J Eng Mech. Div.* **93**(EM6), 37–48 (1967)
30. Coan, J.M.: Large-deflection theory for plates with small initial curvature loaded in edge compression. *ASME J. Appl. Mech.* **18**, 143–151 (1951)
31. Tereszowski, Z.: *Doświadczalna metoda wyznaczania obciążeń krytycznych w płytach*. Archiwum Budowy Maszyn, Tom XVII zeszyt 3, Warszawa (1970)
32. Van der Heijden, A.M.A.: *W.T. Koiter's Elastic Stability of Solids and Structured*. Cambridge University Press, Cambridge (2009)
33. Abaqus HTML Documentation
34. Kubiak, T.: *Static and Dynamic Buckling of Thin-Walled Plate Structures*. Springer, Verlag, London (2013)
35. Zienkiewicz, O.C., Taylor, R.L.: *Finite element method (5th edition) volume 2 – solid mechanics*. Elsevier, Oxford (2000)